ASSESSMENT OF CONSTELLATION DESIGNS FOR EARTH OBSERVATION: APPLICATION TO THE TROPICS MISSION

A Thesis

Presented to the Faculty of the Graduate School

of Cornell University

in Partial Fulfillment of the Requirements for the Degree of

Master of Science in Aerospace Engineering

by

Pau Garcia Buzzi

August 2018

ABSTRACT

The orbit and constellation design process for Earth observation missions is complex and it involves trades between different metrics such as mission lifetime, instrument performance, coverage, cost, and risk among others. In this work, these figures of merit were utilized to support the orbit selection process used during Pre-Phase A and Phase A studies for the NASA-funded Time-Resolved Observations of Precipitation structure and storm Intensity (TROPICS) mission. Thousands of potential constellations were defined, simulated and compared with each other according to different mission coverage requirements. The sensitivity and robustness of figures of merit to various hypothetical operational failures (e.g., loss of one satellite or one launch) was systematically measured. A deployment strategy based on differential drag was described and analyzed. Finally, the orbital lifetime of various architectures was also studied with respect to NASA's 25 years de-orbiting recommendation. The contributions of this work include: (1) an exhaustive analysis of figures of merit commonly used in Earth observation orbit design, including a new metric called Continuous High-Revisit Coverage, which captures the long coverage gaps left by string-of-pearls constellations. (2) A methodology to assess robustness of constellations based on a brute-force disjoint scenario simulation approach (3) Results and recommendations from the mission analysis process for the TROPICS mission.

BIOGRAPHICAL SKETCH

Pau Garcia Buzzi is a second-year aerospace engineering student at the Sibley School of Mechanical and Aerospace Engineering from Cornell University. He received a double Bachelor's degree in industrial and telecommunications engineering from Universitat Politecnica de Catalunya (BarcelonaTech) in Barcelona, Spain. In August 2018, he will graduate with an Master's of Science degree in aerospace engineering. He is particularly interested in the coverage analysis and constellation design for Earth observation missions.

During the past two years, Pau worked under the supervision of his advisor, Dr. Daniel Selva, as part of the orbit and constellation design team of the NASA-funded Time-Resolved Observations of Precipitation Structure and Storm Intensity (TROPICS) mission. This experience provided him with valuable experience and insight into the orbit analysis and design of large constellations of Earth observing satellites. Pau was initially a doctorate student at Cornell University but will transfer to Texas A&M together with his advisor in the Fall 2018 semester, after obtaining his Master's degree from Cornell University.

In the short term, he looks forward to continuing his investigation and applying machine learning techniques to the orbit and constellation design of future space missions. In 3 years, Pau wishes to obtain his doctorate degree at Texas A&M university.

Outside of academics, Pau enjoys outside activities including fitness and running, and he has a lifelong passion for soccer.

This document is dedicated to all my friends and family.

ACKNOWLEDGEMENTS

I would first like to thank my thesis advisor Dr. Daniel Selva for his guidance and useful advice. I would also like to thank my former labmate Dr. Nozomi Hitomi, who was always there whenever I ran into a trouble spot or had a question about my work.

I would also like to acknowledge Dr. Mason Peck as the second reader of this thesis and for being part of my thesis committee.

Finally, I would like to thank my friends and family for supporting me throughout these last 3 years in Ithaca.

TABLE OF CONTENTS

LIST OF TABLES

LIST OF FIGURES

CHAPTER 1

INTRODUCTION

The orbit and constellation design process for Earth observation missions is complex and it involves trades between different metrics such as mission lifetime, instrument performance, coverage, cost, and risk among others. One of the most important trades is arguably the one between the energy (and thus cost) required to put a constellation into the desired orbits and the Earth coverage performance obtained from the resulting constellation. Generally, numerical simulation software, such as AGI's Systems Toolkit (STK), GMAT, or Orekit, is used to compute these coverage metrics in complex scenarios involving multiple satellites and including highly accurate Earth and satellite propagation models. This software calculates the access time intervals for each satellite in the constellation and each point of interest in the user-defined coverage grid on the surface of Earth. These access intervals are the basis for calculation of most coverage metrics or Figures Of Merit (FOM)– words that are used interchangeably in this thesis. Often, several FOM such as mean and maximum revisit time are calculated for a coverage grid containing thousands of points on the surface of the Earth. This may lead to information overload, as it is not trivial how to aggregate all that information into a single number representative of constellation's coverage.

Such coverage metrics need to be traded against cost and risk during Pre-Phase A and Phase A studies to determine the number of satellites and orbital characteristics. In addition, there are other important considerations that must be taken into account in that decision, including the deployment strategy for the constellation, the robustness of the constellation to satellite and launch failures,

as well as mission lifetime and deorbiting.

It is worthwhile to note that, in the experience of the authors, attempting to formulate a multi-attribute decision making problem a priori is challenging because it is hard if not impossible to know a priori the preferences between all these attributes, which would at least in theory require running an Observing System Simulation Experiment for each configuration –which is of course not possible. It is thus more desirable to adopt a more human-driven process, akin to tradespace exploration or design by shopping, in which the main trades and alternatives are discovered at the same time as decision maker preferences are elicited.

With this in mind, the goal of this research is to provide an assessment of the most common FOM used in constellation design, including coverage metrics, but also cost, constellation robustness, deployment strategy and mission lifetime. We use these FOMs to illustrate the orbit selection process used during Pre-Phase A and Phase A studies for the Time-Resolved Observations of Precipitation structure and storm Intensity with a Constellation of Smallsats (TROPICS) mission. The TROPICS mission will monitor the thermodynamics of the troposphere and the precipitation structure for storm systems over the TROPICS regions using a fleet of several LEO MicroMAS-2 CubeSats hosting a payload consisting of a high-performance radiometer that provides different measurements such as temperature and water vapor profiles, imagery for precipitation quantification and cloud ice measurements. The goal is to eventually determine the best candidate architectures considering two major requirements of the TROPICS mission: having a mean revisit time equal or less than 60 minutes over the tropical regions, and distributing the satellites of the constellation

in 3 or fewer planes (due to a constraint on the number of launches combined with the absence of a propulsion system). Different coverage FOM are included in the coverage analysis as well as the quantification of their degradation associated with changes to the original constellation configuration. As part of this goal, the time needed to deploy satellites within a plane is calculated using a differential drag-based strategy exploiting changes in solar panel configuration in eclipse and sunlight period. In addition, orbital lifetime changes are computed for various altitudes and drag area configurations.

The main contribution of this work to the literature is a critical analysis of the different figures of merit commonly used in constellation design and the evaluation of how changes in orbital design parameters such as inclination, altitude, and number of satellites and planes affect these coverage metrics. To the best of our knowledge, this is the first comprehensive effort to characterize the shortcomings of the most commonly used coverage metrics, such as revisit or gap time statistics. Moreover, a new relevant coverage measure called Continuous High Revisit Coverage is defined to account for the fraction of time in which a satellite is either accessed by the constellation or in a gap shorter than a certain threshold, usually set at 120 minutes. The main reason to define this new measure is that other commonly used metrics such as mean revisit time are insensitive to scenarios with undesirable long gaps, which are compensated with numerous short gaps. Also, most papers in the literature only look at optimizing orbital parameters [15, 12, 14, 13, 24, 25, 26, 33, 34, 17], whereas this work also incorporates other important aspects in the orbit selection process, such as robustness and deployment strategies.

The remainder of this thesis is structured as follows: Chapter 2 contains a

review of the most relevant FOM for constellation design and orbit selection in Earth observation missions, including cost and coverage, but also robustness and lifetime considerations. Chapter 3 uses all these metrics to present the TROPICS mission constellation design process, including: a coverage analysis, the degradation of performance due to hypothetical satellite losses in the constellation or launch vehicle failures, the feasibility study of two different deployment strategies, and a mission lifetime assessment. Finally, Chapter 4 presents the conclusions and discusses limitations and opportunities for future work.

CHAPTER 2

FIGURES OF MERIT FOR CONSTELLATION DESIGN

This chapter describes the main FOMs used in the early development stages (Pre-Phase A and Phase A) of Earth observation constellations. Sections 2.1, 2.2, 2.3, 2.4 and 2.5 discuss coverage performance metrics, cost, constellation robustness, lifetime and deployment, respectively. Finally, section 2.6 explains the different parameters to consider when setting up a coverage analysis simulation.

2.1 Coverage

Coverage metrics quantify how well the constellation "covers" the surface of the Earth with its observations. Coverage metrics are usually calculated on a grid of points on the surface of the Earth, by propagating the different spacecraft that compose the constellation for a certain simulation time T, and computing the access time intervals $(ts_{k,i}, te_{k,i})$ in which coverage grid points are seen by any of the satellites, when considering the field of view and imaging concept of the sensors. For every point on the grid k, a coverage gap is the interval of time between the end of access n and the start of access $n+1$: $tg_{k,n} = ts_{k,n+1} - te_{k,n}$. All coverage metrics are calculated from statistics of the access and gap intervals. These statistics are calculated for each point in the coverage grid, but can be aggregated (e.g., averaged out) for all points at a given latitude, or for all points in the coverage definition to obtain, for example, an average revisit time. Of note, other names for access and gap intervals found in the literature are *dwell* and *unattendance time* respectively [11].

There exist a variety of coverage metrics, and it is unclear a priori which ones are best, but the following are some of the most widely used in the literature [32, 15, 13] – all of them are defined for a single point on the grid:

- Descriptive statistics. Minimum, maximum, median, mean, variance and different percentiles of access and/or gap interval duration for a given point of the grid. The most important ones are: maximum revisit time, also known as maximum gap time, which corresponds to the longest gap interval for a single point of the grid. It provides useful worst-case information and it is equal to maximum response (see response time below); and mean coverage gap, also known as mean revisit time, which is the average length of the non-access intervals of a single grid point.
- Percent Coverage (PC). Total time during which a given point of the grid is accessed by at least one satellite in the constellation divided by the total simulation time. It is computed in the following way:

$$PC_k = 1 - \frac{\sum_n tg_{k,n}}{T} \tag{2.1}$$

  where T is the simulation time and $tg_{k,n}$ is the nth gap time for point k in the coverage grid as defined above.
- Mean Response Time. Response time is defined as the time from when a random request is received to observe a point k until we can actually observe it. Note that this is a function of time. If a point k is accessed by a satellite at a given time t, i.e., $ts_{k,n} \leq t \leq te_{k,n}$ for some n, then the response time at that time ($R_k(t) = 0$). But if the point in question is in a coverage gap, i.e., $tg_{k,n} t t s_{k,n+1}$ for some n, then the response time is the time until the end of that gap (until the point is accessed again: $R_k(t) = ts_{k,n+1} - t$). Thus,

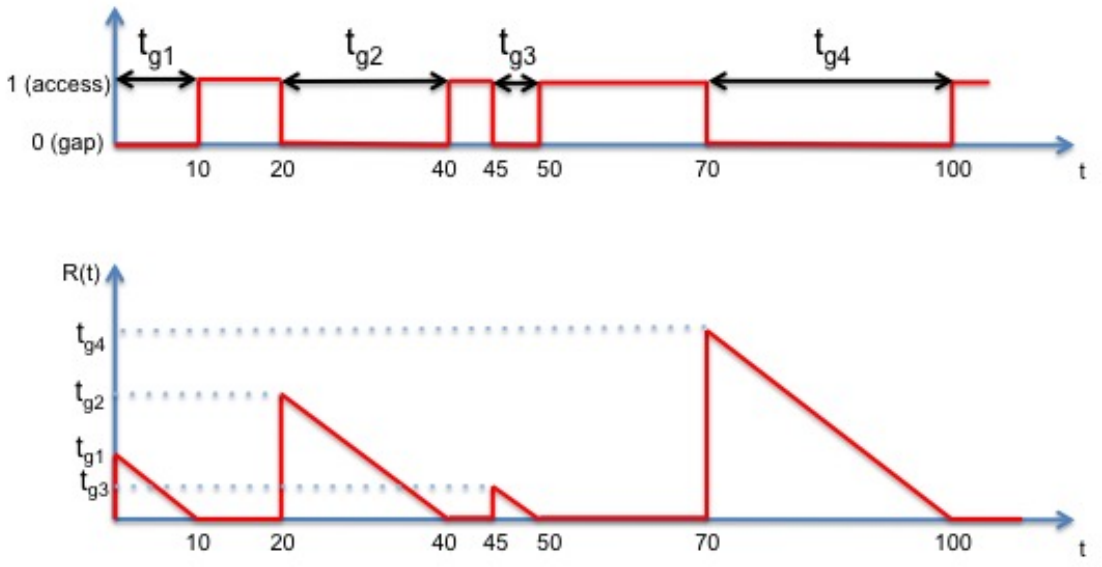

Figure 2.1: Top: Example of gaps and accesses intervals of a particular point on the Earth grid. Bottom: The correspondent response time.

mean response time is defined as the average (integration) of the response time over time. Figure 2.1 shows an example of the response time plot and eq. 2.2 presents how mean response time is computed analytically:

$$R_{k,avg} = \frac{1}{T}\int R_k(t)dt = \frac{\sum_n tg_{k,n}^2}{2T} \tag{2.2}$$

The $\frac{tg_{k,n}^2}{2}$ term comes from the integration (average) of a linear function (the time to next contact). In other words, it corresponds to the area of the different triangles defining the response time curve.

- Time Average Gap. For a given point of the grid k, it corresponds to the time average of the mean gap duration. This figure of merit is very similar to mean response time because the function being averaged (integrated) is the length of the current gap at every time instant $G_k(t)$, which would be 0 in the case of the point being accessed at that particular moment or $tg_{k,n}$ otherwise. Time average gap can be obtained by multiplying the mean

response time by a factor of 2, since the area under the curve we are integrating now corresponds to sum of the area of the rectangles whose area is twice the one of the triangles on the mean response time calculation. It is calculated in the following way:

$$G_{k,avg} = \frac{1}{T}\int G_k(t)dt = \frac{\sum_n tg_{k,n}^2}{T} \tag{2.3}$$

Another metric considered in the TROPICS coverage trade-space analysis that has not been described in the literature is what we called the Continuous High Revisit Coverage (CHRC), which is defined as the percentage of time where point k is either in visibility or in a gap shorter than a threshold t_{hold}. It is computed in the following way:

$$CHRC_k = 1 - \frac{\sum_n (tg_{k,n} \geq t_{hold})}{T} \tag{2.4}$$

Other coverage metrics found in the literature are total time of coverage over a region, and access to daytime and nighttime coverage [29]. Total time of coverage over a region gives the same information as the percent coverage but for a region (a set of points) instead of a single point. Thus, if any point in the region is observed, the region is considered observed. Zhang et al. [35] define Coverage Rate of sampling points as the ratio between the number of time steps where the point was in access and the total number of time steps. Note that this metric is less precise than percent coverage as defined above, since coverage state is only checked at constant time steps, and thus the exact start and end times within the time steps of the different accesses are ignored. The smaller the time step, the closer coverage rate will be to percent coverage.

Of note, many other coverage metrics exist in the literature that are specific to intelligence, surveillance and reconnaissance tasks. Examples are analysis

time, target leakage, target coverage frequency and target ghost time [11]. These metrics were left out of scope of this thesis, which deals with observation of the Earth system's geophysical parameters, as opposed to dynamic targets.

So far, several relevant access/gap metrics have been listed, which are computed for a given point on the grid. For many purposes, such as using coverage metrics as objectives in optimization problems or when conducting a trade space exploration of several constellation configurations, it is convenient to condense information for different points of the grid into a single quantity that summarizes the coverage of an architecture or constellation. For example, statistics of single-point metrics can be aggregated across a region of interest, be it worldwide (Global), or regional (e.g., tropical regions, "cold" regions, or continental US). Another way of condensing information is to do a weighted average of the metric values for different points in the grid, for example weighting average revisit times by the cosine of the corresponding latitude (AWART) [15], which effectively makes tropical regions more important than cold regions. More generally, latitude-weighted metrics should reflect the importance of different latitudes to the mission objective at hand. For example, as the main objective of TROPICS is to monitor extreme weather events around the tropics, we weigh latitudes proportionally to the storm frequency data shown in figure 2.2.

Coverage for narrow-swath instruments

Narrow-swath instruments such as lidars and certain radars and high-resolution imagers often require special considerations when assessing coverage. Indeed, for these missions, it is often unfeasible to attempt to achieve global coverage for all longitudes. Instead, such sensors are put on repeat ground track

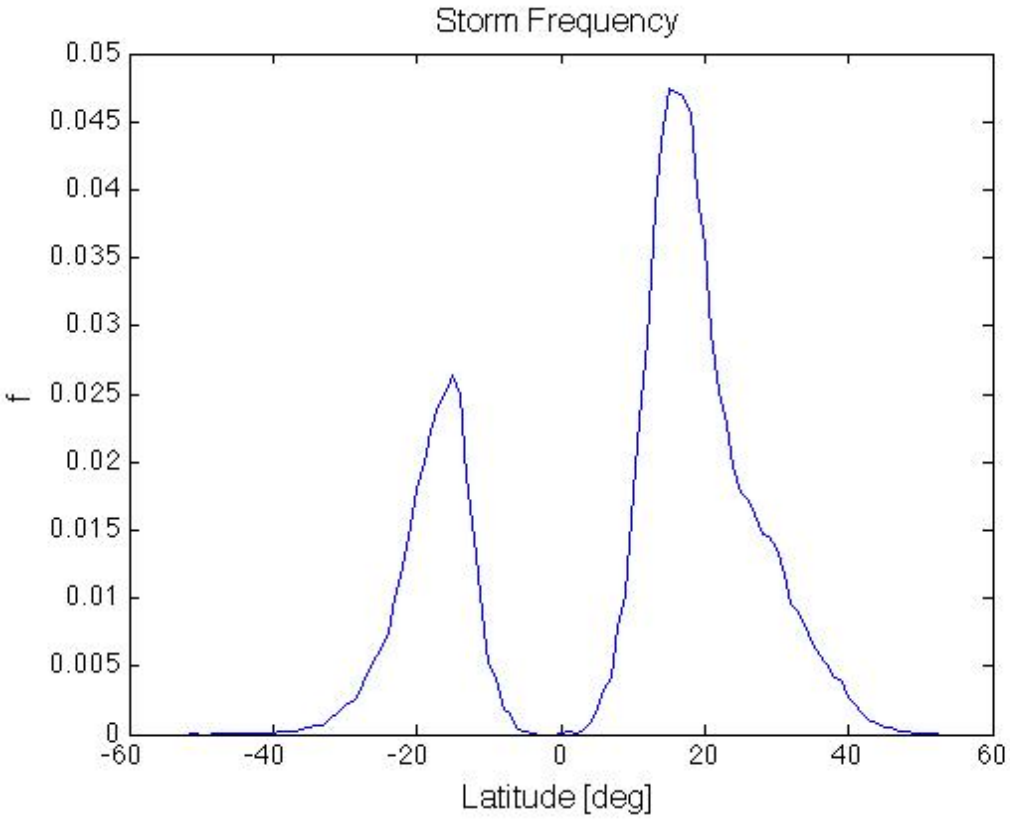

Figure 2.2: Storm frequency vs latitude. These values were used as latitude weights to compute latitude-averaged coverage metrics.

orbits that guarantee a certain revisit time (equal to the repeat ground track period) for the regions covered, but leaves some regions out. Thus, if we attempt to calculate the metrics defined in the previous subsection, we observe a strong dependency on the total simulation time, since the gap time for all non-visited points is equal by default to the total simulation time.

In these cases, the first metric that is important to capture is the total area or percentage of the earth's surface that is being covered. In general, for a single satellite, there is a trade-off between achieving good coverage (which requires a large repeat period) and achieving good revisit time within the area covered (which requires a small repeat period). Once this trade-off is understood, the

metrics defined in the previous subsection can be used only on the regions visited by the sensor.

2.2 Cost

Naturally, coverage of a constellation is traded against number of satellites and ultimately cost. Cost can be considered as an objective to be minimized, or as a constraint to satisfy. Access to Earth orbit for small satellites, and specifically the cost and availability of launch services, is still a big problem nowadays and arguably the most significant threat to the growth of concepts based on large constellations of small satellites [6].

While ideally one would like to incorporate cost in these trades, cost is very challenging to estimate, especially during Pre-Phase A studies where there is a lot of uncertainty. Hence, proxies are often used instead of cost.

Wertz [32] use the mission ΔV budget to define the Orbit Cost Function (OCF), which allows us to estimate the relative cost of putting a spacecraft into a given orbit relative to the cost of putting it into a 185 km circular low-Earth orbit. Specifically, the OCF is defined as the ratio of the mass delivered in a 185 km altitude circular orbit to the mass delivered in mission orbit. It can be seen as a multiplier to obtain the cost of putting a spacecraft into its mission orbit from the cost of putting the spacecraft in LEO, which can be estimated using historical launch vehicle cost data.

The cost model used in this work tries to capture the effect in cost of the main design decisions such as the altitude, inclination, the number of satellites

in the constellation, and the way these satellites are distributed among one or several planes. The total cost of the mission is composed of constellation cost and launch cost as shown in equation 2.5:

$$Cost = C_{Launch} + C_{Const} \tag{2.5}$$

As shown in equation 2.6, the constellation cost is computed multiplying the number of total satellites by the cost of a single satellite, 1 M$, therefore assuming no learning curve. The launch cost is calculated multiplying the cost of a single launch by the number of planes in the constellation as seen in equation 2.7.

$$C_{Const} = n_{Sat} \cdot C_{Sat} \tag{2.6}$$

$$C_{Launch} = n_{Planes} \cdot C_{LV} \tag{2.7}$$

In doing so, the assumption of needing an extra launch vehicle for every additional plane in the architecture is made. This is a reasonable assumption since many small satellites do not have propulsion capabilities to do expensive out-of-plane orbit maneuvers such as changing RAAN [7]. A possibility not considered in this work is the ability of the upper stage of the launch vehicle to make plane changes and deliver satellites to multiple planes. Therefore, a single launch vehicle can only deliver payloads to a given orbital plane.

In our cost model, the proxy used for launch cost is the cost of the propellant needed to put the spacecraft into the desired mission orbit. The reason behind making this approximation is the difficulty to obtain accurate pricing informa-

tion for launch services, which also depends on purely commercial considerations. Our strategy, based on energy computations, makes this estimate independent of the pricing strategy while still being a reasonable proxy for launch cost.

The amount of propellant needed is computed in several steps. First, the ΔV required to go from the launch site to the desired altitude h and inclination i is computed as shown in Eq. 2.8.

$$\Delta V_{h,i} = \Delta V_{0-400km} + \Delta V_{400km-h} + \Delta V_{28.7^\circ - i} \tag{2.8}$$

where $\Delta V_{0-400km}$ is the ΔV required to go from altitude 0 to a LEO of 400km and 28.7° inclination –which depends on the launch site among other things, and is assumed to be a known constant of 10,000 m/s. $\Delta V_{400km-h}$ is the ΔV required to go from 400km to to the desired altitude $h > 400km$, which is computed using a Hohmann transfer. Finally, $\Delta V_{28.7^\circ - i}$ is the ΔV required to go from an inclination of 28.7° to to the desired inclination i, assuming a simple plane change maneuver, which is calculated as:

$$\Delta V_{28.7^\circ - i} = 2 \cdot v_h \cdot \sin\left(\frac{|i - 28.7|}{2}\right) \tag{2.9}$$

where v_h is the the orbital velocity at altitude h.

In our cost model, we considered both dedicated launch and ridesharing/piggybacking options, often used for CubeSats [8]. Dedicated launches provide more freedom to the customer to select the destination orbit and the launch date but are more costly than ridesharing/piggybacking options, which

provide less (or no) flexibility in choosing orbits and mission schedule.

Therefore, the final launch vehicle cost is given by:

$$C_{LV} = \min(Cost_{dedicated}, Cost_{rideshare}) \tag{2.10}$$

To compute the dedicated and rideshare launch costs, the Electron launch vehicle from Rocket Lab was considered [20], as a good representative of launch services specializing in small satellites. The rideshare alternative was only possible if the sum of payload mass (m_{pload}) and initial payload (m_{pload0}) was less than the maximum payload mass ($m_{ploadmax}$), a value that changes depending on the final orbital altitude and which was found in the Rocket lab's user guide. The assumption of an initial payload of 75kg was made, corresponding to half the maximum possible payload mass that the rocket can carry to a 500km orbit.

Using the rocket equation, $\Delta V_{h,i}$ is translated into kg of propellant required for the launch. For the dedicated launch option, the mass of propellant is computed the following way:

$$m_{propD} = (m_s + m_{pload}) \cdot e^{\left(\frac{\Delta V_{h,i}}{gI_{sp}}\right)} - m_s - m_{pload} \tag{2.11}$$

where m_s is the predefined structure mass of the launch vehicle, 1200 kg, m_p is the mass of the payload ($n_{sat}/n_{planes} \cdot 6kg$), g is the standard gravity constant and I_{sp} is the specific impulse of the propellant, 300 s.

On the other hand, for the rideshare option, the mass of propellant needed is assessed by considering the difference between the propellant needed to put ($m_{pload0} + m_{pload}$) into orbit and just putting (m_{pload0}) into orbit:

$$m_{propR} = (m_s + m_{pload0} + m_{pload}) \cdot e^{\left(\frac{\Delta V_{h,i}}{g I_{sp}}\right)} - m_s - m_{pload0} - m_{pload} - (m_s + m_{pload0}) \cdot e^{\left(\frac{\Delta V_{h,i}}{g I_{sp}}\right)} - m_s - m_{pload0} \quad (2.12)$$

Finally, this amount of propellant is translated into dollars using eq. 2.13 and eq. 2.14 for the dedicated and rideshare launches, respectively:

$$Cost_{dedicated} = 4.35M\$ + c_p \cdot m_{propD} \quad (2.13)$$

$$Cost_{rideshare} = c_p \cdot m_{propR} \quad (2.14)$$

where c_p is the specific cost of propellant, assumed to be 17 \$/kg. It is important to note that, for the dedicated launch option, there is an extra cost constant of 4.35 M\$ that corresponds to the cost of building the rocket specifically for our mission. Since the Rocket Lab's dedicated launch services start roughly at 5 M\$, the cost of building the rocket was assessed by subtracting to 5 M\$ the cost of putting the maximum possible payload (150 kg) in an orbit of 500km and 30 degrees inclination.

2.3 Robustness / Operational Risk

Another important issue to take into account when designing a satellite constellation is risk of spacecraft and launch vehicle failure, since some constellations may be more robust to operational risks than others. There are many sources of risk for space missions. For instance, the increasing quantity of space debris

is a cause of concern since tiny projectiles can damage satellites due to the high collision velocity [28]. This is especially problematic for higher altitudes where the density of the atmosphere is low and atmospheric drag is not capable of removing the abundant small debris. Other common sources of mission failure include communications or power subsystem problems, such as failure deployable components, and launch vehicle failure leading to complete spacecraft loss in the worst case, and reduction in mission lifetime or performance and/or large effort and cost for mission recovery in the best case [5].

Most published work on constellation design focuses on achieving a certain level of performance, usually set by mission requirements, with the nominal constellation, assuming 100 % satellite availability and not taking into account hypothetical spacecraft failures. However, constellations with similar nominal performance may have very different levels of robustness to spacecraft or launch failure, and therefore it is important to consider robustness in constellation design. A simple way to asses the extent to which constellation robustness is to evaluate if the constellation can still accomplish goals and mission requirements in the event of the loss of any single or multiple spacecraft [10, 22]. Naturally, the smaller the changes in performance after losing spacecraft in the constellation, the larger its robustness –i.e., its capacity to resist coverage degradation.

In [9], a comparison of cost and performance– or utility– between monolithic and fractionated spacecraft architectures accounting for failure and replacement of spacecraft in the system is done using Markov models.

In this work, satellite and launch vehicle failures were modeled as a finite sequence of independent and identically distributed binary random variables–

i.e. a Bernoulli process. Each satellite and launch vehicle in the constellation can only take two values to indicate whether the satellite or launch vehicle fail or not before the mission design lifetime. Each variable in the sequence is associated with a Bernoulli trial or experiment. In this work, the probability of launch vehicle failure and satellite failure before the mission lifetime are assumed identical and equal to ($P_f = 0.1$) so the probability of success for each is ($P_s = 1 - P_f = 0.9$). Since each satellite and each launch vehicle can either fail or not and the number of launch vehicles equals the number of planes, there are a total of $2^{n_{sat}+n_{planes}}$ possible states for the system. A brute-force approach was used to calculated the robustness of each constellation, so each of these states was enumerated and evaluated. Specifically, for each state, the probability of being in that state and the corresponding coverage performance were calculated. Given a representation of the state as a bit-string of $N = n_{sat} + n_{planes}$ elements ($X = [x_1, ..., x_N]$), where $x_i = 0$ if element i fails and $x_i = 1$ otherwise, the probability of each state can be computed as follows:

$$P(X) = \prod_{i=1}^{N} P_s^{x_i} \cdot P_f^{1-x_i} = \prod_{i=1}^{N} P_s^{x_i} \cdot (1 - P_s)^{1-x_i} \tag{2.15}$$

As mentioned earlier, this equation assumes that all satellite and launch vehicle failures are independent. If failures are not independent (e.g., in the presence of common cause failures), then conditional probabilities must be used, and a similar expression can be obtained for certain simplified cases, but this is left out of the scope of this thesis.

In terms of calculating coverage performance, note that no new simulations are required once the architecture with all its elements has been evaluated. Indeed, if the accesses corresponding to each individual spacecraft in the constel-

lation are stored separately and then merged to calculate the coverage metrics, one can simply choose the subset of accesses corresponding to the satellites that did not fail in that state, merge them, and compute the corresponding coverage metrics.

Once probabilities and coverage metrics are available for all possible system states, probability density functions (PDFs) and Cumulative distribution functions (CDFs) for the different coverage metrics can be obtained to evaluate constellation robustness (using, for example, the mean, the median, or any other percentile of the CDF).

2.4 Lifetime

Spacecraft lifetime is another relevant metric to consider in constellation design, especially for satellites in very low orbits (500km or lower), which can suffer from rapid orbital decay due to high atmospheric drag [25]. Furthermore, for CubeSats without propulsion subsystems, where orbit maintenance becomes more challenging or impossible, lifetime is a crucial parameter for mission success. On the other hand, if satellites are placed in higher orbits where drag is negligible, CubeSats without alternative de-orbiting capabilities such as propulsion would orbit almost indefinitely around the Earth after the satellite's mission life, increasing space debris. For that reason, NASA's End of Mission Considerations [19] recommend to set a constellation altitude and area-to-mass ratio so that reentry by atmospheric drag is ensured to occur within 25 years after the end of mission. Given that many CubeSats don't know their operational orbit until well after the design phsae, this is a challenging requirement.

Another important parameter that significantly affects orbital decay besides altitude and area-to-mass ratio is the solar cycle. With increasing solar activity, the atmospheric density and thus drag increase significantly, lowering satellite's lifetime. For that reason, and specially for short space missions, it is relevant to assess the sensitivity of mission start time to orbital decay with the ultimate goal of tuning this parameter to obtain desirable values of lifetime.

While accurate calculation of deorbiting requires numerical propagators, analytical approximations exist that can be used to iteratively calculate mission lifetime. For example, [32] provides the following equations to account for the effect that drag has on satellite decay for circular orbits:

$$\Delta a_{rev} = -2\pi \left(C_D \frac{A}{m} \right) \rho a^2 \tag{2.16}$$

$$\Delta P_{rev} = -6\pi^2 \left(C_D \frac{A}{m} \right) \rho a^2 / V \tag{2.17}$$

$$\Delta V_{rev} = \pi \left(C_D \frac{A}{m} \right) \rho a V \tag{2.18}$$

where Δa_{rev}, ΔP_{rev} and ΔV_{rev} are the changes in semi-major axis, orbital period and satellite velocity per revolution/orbit, respectively. C_D is the dimension-less drag coefficient of the satellite, A is the cross-sectional area (perpendicular to the velocity vector), m is the satellite mass, a is the current semi-major axis, V is the current satellite velocity and ρ is the atmospheric density, which as mentioned is very sensitive to altitude and solar activity. Note that both v and ρ depend on altitude and thus on a. Using these three equations iteratively, an estimation of

satellite lifetime can be assessed by observing the changes in altitude and orbital period in time. However, in this work, all lifetime calculations have been performed propagating the spacecraft using a high precision propagator available in Orekit, keeping track of its semi-major axis and stopping the propagation at an altitude equal or lower than 120 km. This approach, despite being more computationally expensive, allows us to take into account other aspects such as oblateness of the Earth and use sophisticated density models available in in the Orekit software library.

2.5 Deployment

As mentioned in section 2.2, often small satellites must be launched as secondary payloads due to budget constraints. This fact sometimes restricts their deployment in the required/ideal constellation geometry [27]. For example, even separation of satellites in mean anomaly within a plane and even separation in RAAN across planes are usually desirable to minimize maximum revisit times, but instead of that, a secondary launch may mean reduced or no separation within or across planes. For small satellites without propulsion capabilities, drag-based deployment strategies are often considered to reach some level of spacing between satellites [23, 2, 30, 31, 18, 1]. The strategies make use of asymetries in the geometry of the spacecraft and/or deployables such as solar panels to change the drag of each individual spacecraft, which can be used to adjust the relative phasing between them. These strategies have been demonstrated on orbit by the CYGNSS mission. CYGNSS consists of 8 microsatellites which, once deployed by a single launch vehicle in a 500km altitude orbit, were evenly spaced in mean anomaly (45 degrees from each other) in the same orbit using

a differential drag technique [16]. A similar approach was studied for TROPICS and is described below. Of particular interest is the time required to reach the desired constellation geometry (e.g., even separation in mean anomaly), as this can be an important fraction of the mission lifetime. This metric– which we called time to operational orbit– is very significant since some deployment strategies can take years to complete, limiting mission operational lifetime.

Time to operational orbit can be estimated analytically using eq. 2.16,2.17 and 2.18 provided in subsection 2.4. Indeed, an analytical estimate of the variation of altitude and orbital period per revolution for the different satellites placed in the same orbital plane can be obtained. Next, using the difference in orbital period between a pair of satellites, it is possible to keep track of their relative mean anomaly variation per revolution. However, similarly to what we did for lifetime computations, this analytical approach was not used and, instead, numerical propagation of the different satellites was used to keep track of the separation of satellites during mission deployment.

2.6 Simulation set up

Fast analytic approximations for evaluating Earth coverage are available [32] for several parameters such as Footprint Area (FA), which is the area of the Earth surface that an instrument is seeing at any moment, Instantaneous Access Area (IAA), which is all the area that an instrument could potentially see at any moment, Area Coverage Rate (ACR), which is the rate at which an instrument is accessing new Earth surface or Area Access Rate (AAR), which defines the rate new Earth surface Earth surface is coming into the instrument's access

area. However, these approximation models do not include aspects such as the oblateness of the earth, the rotation of the Earth underneath the satellite orbit, orbit eccentricity, or the assessment of coverage by more than just a single satellite. These analytic approximations were not used in this work and, instead, numerical simulation was performed to obtain additional details by computing the different metrics listed in subsection 2.1, which are not assessed by any analytical model.

The main issues to take into account when setting up a coverage analysis simulation are:

- The number and the distribution of the points in the coverage grid. The greater the number of points, the better the spatial resolution of the results but, of course, the longer the simulation time;
- The simulation time. It must be long enough to at least capture several orbits of the different satellites, and ideally any relevant seasonal effects, so that the results obtained are representative of the whole mission life;
- The characteristics of the sensors. Results on the size and shape of the sensor field of view;
- The time step of the propagation. It should be selected together with the coverage grid resolution and the sensor field of view. Specifically, the time step should be chosen so that there are no spatial gaps in sensor footprint swath between two consecutive time steps, since that could lead to artificially missing a grid point access;
- Fidelity of the propagation. The simulations can be run using models of various complexity and fidelity. Logically, the more complex the model, the longer the simulation time. For satellite propagation, Keplerian, J2,

and numerical models can be considered. The Keplerian propagator only takes into account the symmetric central body force. The J2 propagator adds to that first model the J2 zonal harmonic coefficient contribution to account for Earth's oblateness, which allows to model sun-synchronous orbits among other things. Finally, high precision numerical propagators incorporate J2 effects, drag (we used the DTM2000 atmospheric model [4]), third body effects of the Sun and Moon, and solar radiation pressure disturbances to the propagation of the satellite.

CHAPTER 3

APPLICATION TO TROPICS MISSION

This section describes the process followed to explore various constellation design alternatives for the TROPICS mission, using the FOMs introduced in the previous chapter.

3.1 Simulation parameters

All the simulations performed were run using Orekit, a free low-level space dynamics library written in Java that provides basic tools and accurate and efficient low-level components for the development of flight dynamics applications. On top of the Orekit library, we built the capability to run coverage analysis for the different purposes of this work. Our code is open source and can be downloaded from GitHub [21].

A grid of 9° granularity in latitude has been used in this work. Moreover, the number of points at each latitude has been chosen to be proportional to the cosine of the latitude to obtain equal horizontal distances between points. Therefore, fewer points are placed in higher latitudes to avoid statistically weighting more the poles in the global coverage metrics. This is especially relevant for the TROPICS mission, which focuses on keeping track of storms in the tropical regions and there is less interest in coverage of the poles. This results in a grid of 512 points around the Earth surface.

The simulation time for each scenario was set to 1 week, enough to capture about 100 orbital periods for the highest orbits considered of 800km (which

corresponds to about 109 orbital periods at 400km). Clearly, one week is not enough to capture seasonal effects. However, in this case study, we cared mostly about coverage metrics, and after performing a few simulations with a 1 year duration and comparing the results with the ones obtained with just 1 week long simulations, the biggest differences in coverage metrics were found to be around 20% for constellations at 400km (where drag is very large) and 5% or lower for altitudes of 600km or higher, which was judged acceptable;

In this work, a rectangular field of view (FOV) was used and the payload's swath was set to scan out to +/- 57°. The TROPICS payload is a high-performance radiometer that rotates about the velocity vector at 30 rpm and it has a FOV of about 5°. The rectangular FOV used is an approximation of TROPICS' payload characteristics: the cross-track FOV was set to the max value in terms of incidence angle for observations, and the along track FOV was set together with the simulation time step and the spacing between points in the Earth grid so that no gaps were artificially generated in the along-track direction;

A high precision numerical propagator that incorporate J2 effects, drag, third body effects of the Sun and Moon, and solar radiation pressure disturbances to the propagation of the satellite was used in this work and all the characteristics from the TROPICS CubeSats were considered, setting a satellite mass of 6kg, a solar area of 0.058m^2 and a nominal drag area of 0.075m^2.

3.2 Coverage Tradespace Exploration

The main decisions to assess the final TROPICS constellation of satellites configuration were the total number of satellites, the number of planes, and the orbit

altitude and inclination. To aid in decision making, a set of constellations were simulated containing a full factorial enumeration of circular Walker constellations up to 16 satellites distributed in 3 or less planes, and including altitudes of 400km, 500km, 600km, 700km and 800km, and inclinations of 30°, 51.6° (the ISS inclination, because there are many launch opportunities to that orbit), 90°, and Sun-Synchronous Orbits (SSO). Therefore, hybrid configurations with satellites at different altitudes and/or inclinations were not analyzed. Potentially, however, by using constellations with planes of different inclinations, we could obtain better coverage performance than just considering Walker constellations.

In order to select the 'preferred' constellation for the TROPICS mission, we describe below a process that is more linear or sequential than the one followed in reality, but the main arguments from the actual process are all present. We start by determining the inclination of the satellites in the constellation considering the main goal of the TROPICS mission, which is monitoring hurricanes and storms located in lower latitudes. Results show that, when looking at aggregate coverage metrics conditioned on inclination, 30deg is the preferred value of inclination. Next, altitude is considered, and the decision of 600km is made as a compromise between spatial resolution, coverage performance, lifetime, and cost. Once both inclination and altitude are fixed, the number of satellites in the constellation is chosen to meet the mission's coverage performance threshold while minimizing cost and considering constellation robustness to hypothetical failures. Finally, the number of planes decision is made to optimize the constellation's response time and minimizing the longest gaps of coverage while subject to the constraint of having a maximum of three launches.

In order to study the trades between the different constellations simulated,

different coverage and performance metrics were considered: weighted mean revisit time, weighted median revisit time, weighted 90th percentile of revisit time, weighted maximum gap time, weighted mean response time, weighted CHRC and cost. All metrics were latitude-weighted using the information presented in Figure 2.2 from section 2. For constellations with inclination of 30 degrees, the weights corresponding to the latitudes larger than 36 degrees were set to 0. The reason behind this modification is that, even though the weights were already very small, at this field of view, higher latitudes are not reachable from 30-degrees inclination constellations and the weighted average of the different metrics were significantly affected by 'fake' gaps of non-accessed latitudes, whose length was the entire simulation time.

Additionally, another important metric to consider was the instrument spatial resolution, which for a microwave radiometer with a circular aperture is given by:

$$SR = 1.22r\frac{\lambda}{D} \tag{3.1}$$

where r is the range or distance between the instrument and the Earth grid point, which for circular orbits is equal to the altitude divided by the cosine of the off-nadir angle, and λ and D are the wavelength and aperture of the instrument, respectively. The first portion of the MicroMAS-2 radiometer payload uses eight channels uniformly spaced in frequency from approximately 114 to 119GHz and one window channel at 108-109GHz. The instrument has a single aperture of approximately 7cm [3], which leads to different values of spatial resolution for the different channels.

Whereas high altitudes and high numbers of satellites are preferred from a coverage perspective, the cost and spatial resolution metrics will penalize these

architectures, thus establishing a basic trade-off. Indeed, for higher altitudes and number of spacecraft, the satellites will have a larger ground swath and, therefore, accesses and gaps will be longer and shorter respectively; at the same time, these architectures will have worse spatial resolution and will be more expensive since the launch vehicle cost will grow with altitude and as number of satellites increases.

Another factor that we sought to study is the influence of the placement of the satellites into different planes in gap time distributions. For example, what are the differences in gap time distributions, for a constellation with 12 satellites in the same orbital plane vs the same 12 satellites in 3 or 4 planes equally spaced in RAAN?

Figure 3.1 shows a box-plot comparison of the latitude-weighted mean, median, 90th percentile and maximum revisit times for the different inclination groups considering all 940 constellations. Note that in each of these boxplots, there are 235 constellations with different values of altitude, number of satellites, and number of planes. The 30° inclination architectures provide significantly better coverage for the tropical regions, going from a weighted mean revisit time mean of 101 minutes for SSO to 45 minutes for 30°.

Mean revisit time and high percentiles of revisit times are the metrics that change the most when varying the inclination of the orbits, whereas the weighted median revisit time is not very sensitive to inclination changes. These results are also exemplified in figure 3.2, where we plot the CDFs of 4 specific constellations out of the 940, all with 12 satellites distributed in 3 planes and 600km altitude (the values that were eventually selected as the baseline architecture) but inclinations of 30° , 51.6°, 90° and SSO respectively. All curves show

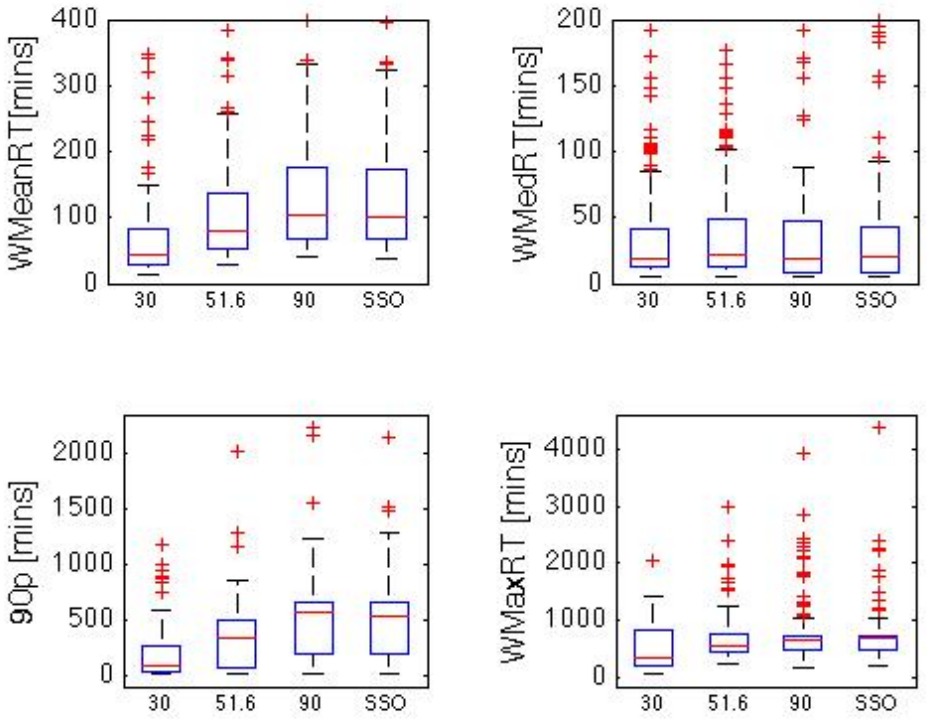

Figure 3.1: Comparison of the latitude weighted mean, median, 90th percentile and maximum revisit time for the different inclinations of study

similar values of median revisit time and low percentiles of revisit times but they diverge in the higher percentiles of revisit times. All the architectures with an inclination different from 30° were filtered and ruled out for further analysis as they are more costly and do not provide any better coverage performance in this problem than the 30° ones.

Figure 3.3 shows the plot of the weighted mean revisit time with respect to the mission cost for all the architectures with 30° inclination. Four different curves corresponding to the different altitude cases are detected. Architectures at 600km offer a good trade between cost, coverage performance and spatial resolution. Going from an altitude of 400km to 600km, we decrease significantly

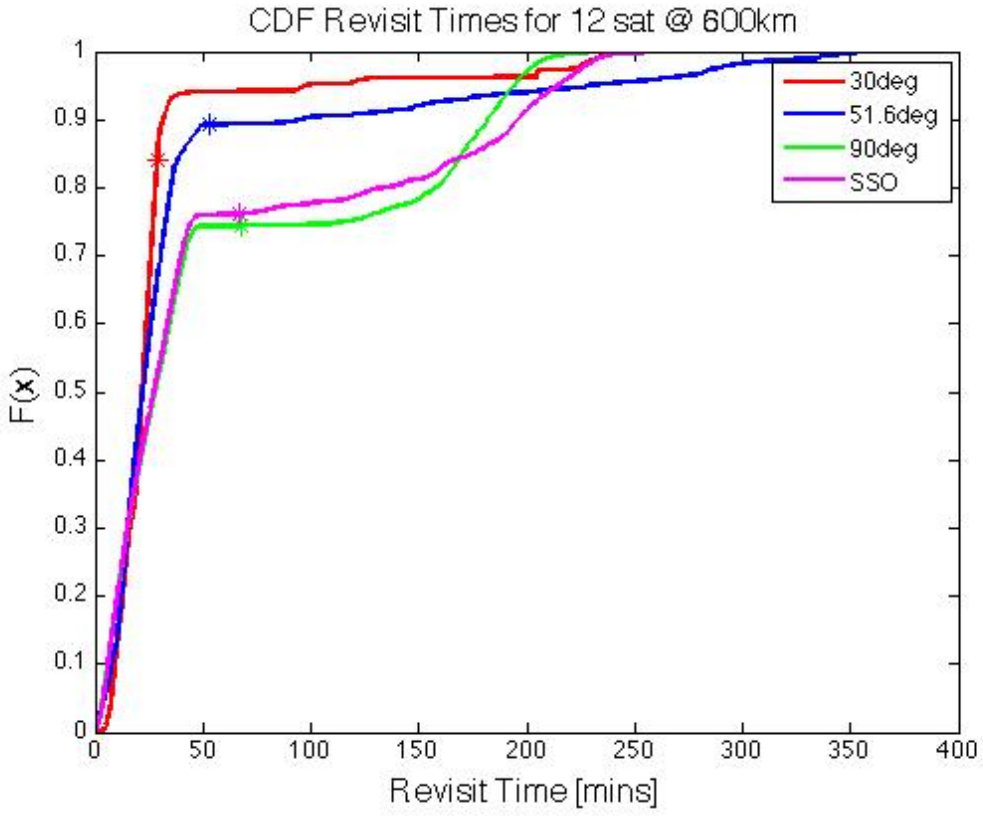

Figure 3.2: Comparison of the CDFs of 4 Walker constellations of 12 satellites at 600km altitude and different inclinations. The markers (*) show the values of weighted mean revisit time for each of the four configurations

the weighted mean revisit time. Moreover, the coverage performance at 600km is good enough for the mission purposes as we can easily get weighted mean revisit times of less than 60 minutes and, increasing the altitude of the architecture would worsen both cost and spatial resolution. In addition, the 600km altitude is high enough to avoid an exceedingly short mission lifetime to do drag, but still low enough to be able to satisfy NASA's recommendation to deorbit within 25 years of the end-of-life.

With a 30° inclination and 600km altitude selected, the number of satellites in the TROPICS constellation and the number of planes in which to distribute the satellites were the following design decisions to make. In figures 3.4 and 3.5,

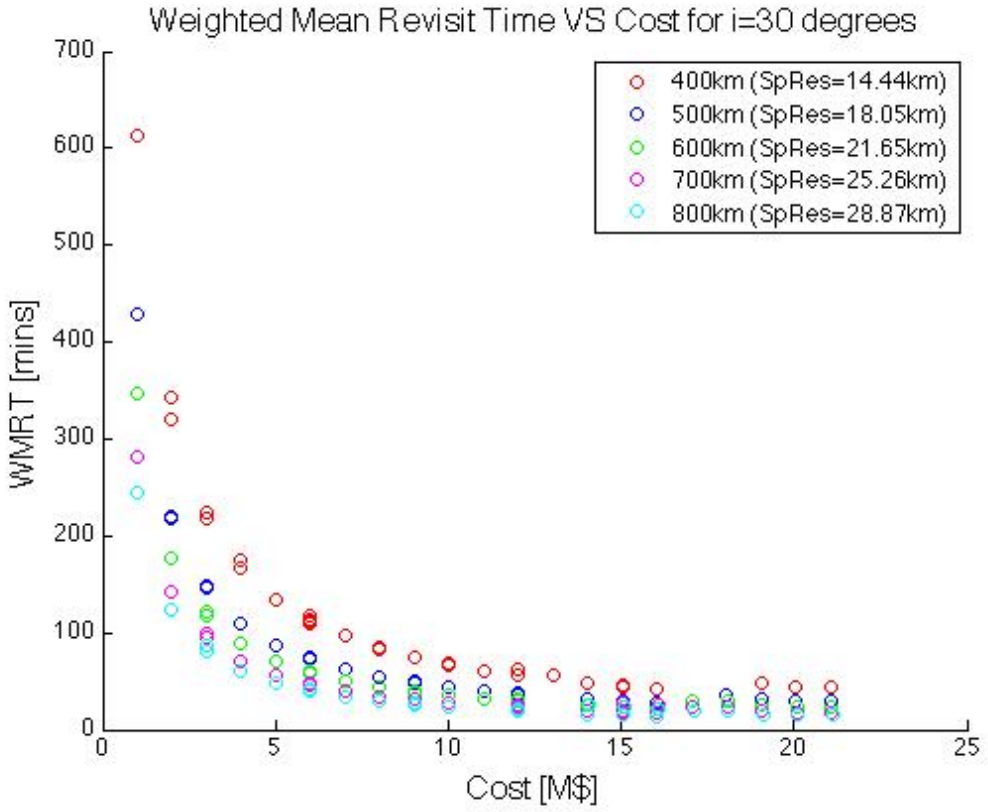

Figure 3.3: Latitude weighted mean revisit time vs cost for all 30 degrees simulated constellations

the number of satellites required to achieve certain values of weighted mean and median revisit times can be obtained, respectively. However, increasing the number of satellites will also increase cost, as expected and seen in figure 3.6. Therefore, the minimum required number of satellites will be selected unless risk/robustness factors are considered. In other words, a more robust constellation design may be considered to account for hypothetical satellite losses that would potentially decrease coverage performance. For this reason, at this point in our constellation tradespace analysis, we decided to consider two different candidate constellations:

- Threshold architecture, formed by 6 satellites, which allows us to meet the

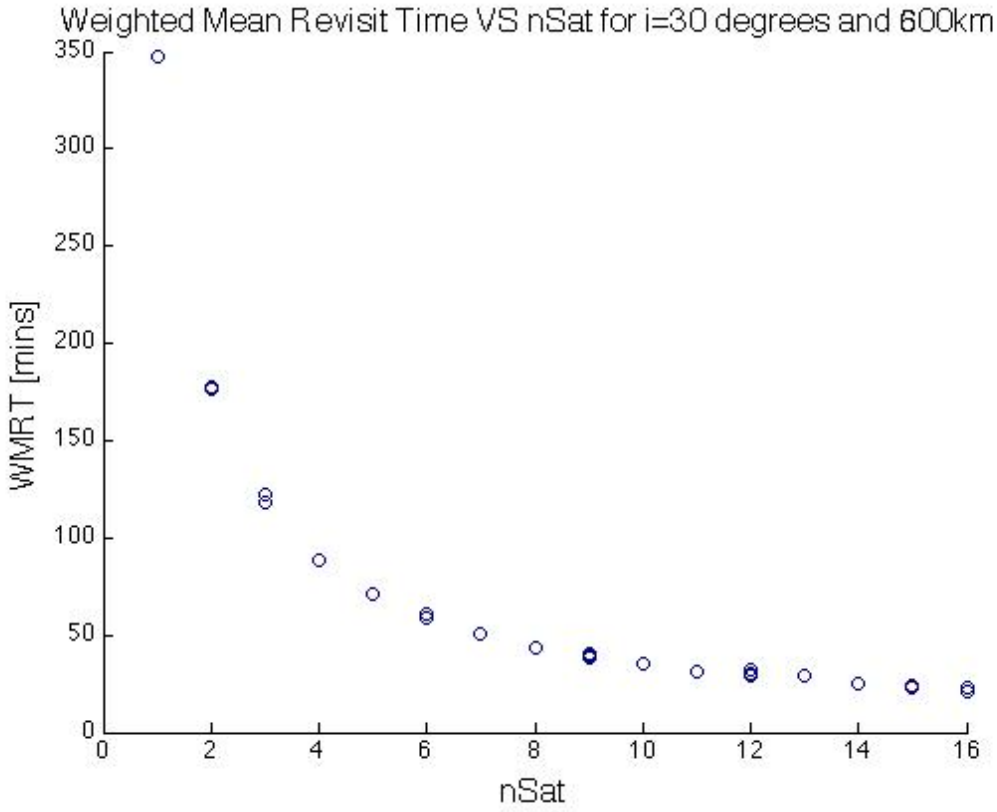

Figure 3.4: Latitude weighted mean revisit time vs nsat for all constellations with 30° inclination and 600km altitude

main mission coverage requirement to have a weighted mean revisit time equal or less than 60 minutes with the lowest number of satellites possible. Figure 3.4 shows that with 6 satellites, we obtain a weighted mean revisit time of 59 mins.

- Baseline architecture, formed by 12 satellites, which not only allows us to meet the mission coverage requirements (weighted mean revisit time goes down to 29 mins) but also provides a high level of robustness both for a hypothetical LV failure or satellites losses in the constellation to still meet the mission coverage requirements, as it will be shown later in this section.

Finally, the impact in coverage metrics of choosing one vs several planes in

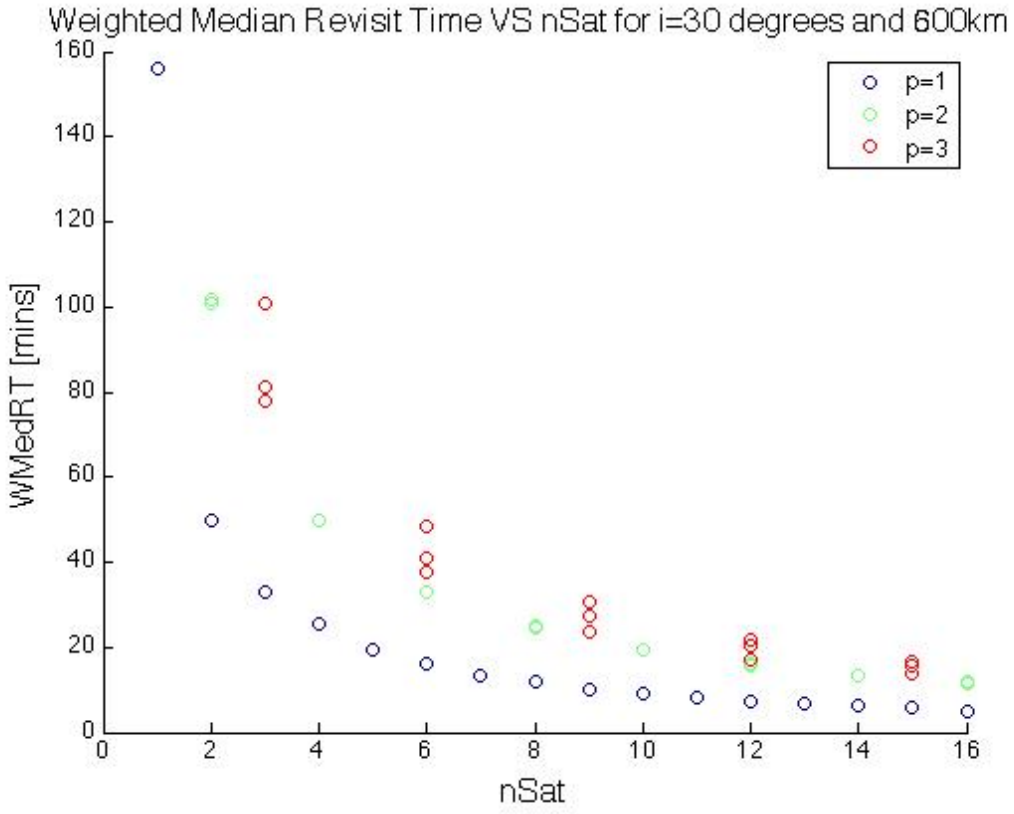

Figure 3.5: Latitude weighted median revisit time vs nsat for all constellations with 30° inclination and 600km altitude

which to distribute all the satellites was assessed. It was found that median and high percentiles of revisit times are the metrics that change the most when varying the number of planes design variable, whereas the weighted mean revisit time is barely affected. This results are illustrated in 2 plots: In figure 3.7, a comparison of the CDFs of 3 different architectures is shown, all with 12 satellites at 600km altitude and 30° inclination distributed in 1, 2 and 3 planes (local analysis); In figure 3.8, weighted mean, median, maximum and 98th percentile gaps are compared for different number of planes including all constellations at 600km and 30° inclination (global analysis). Both the global and local analysis suggest that median and lower percentiles of revisit times appear to be slightly better for architectures of one plane whereas higher percentiles (i.e.,

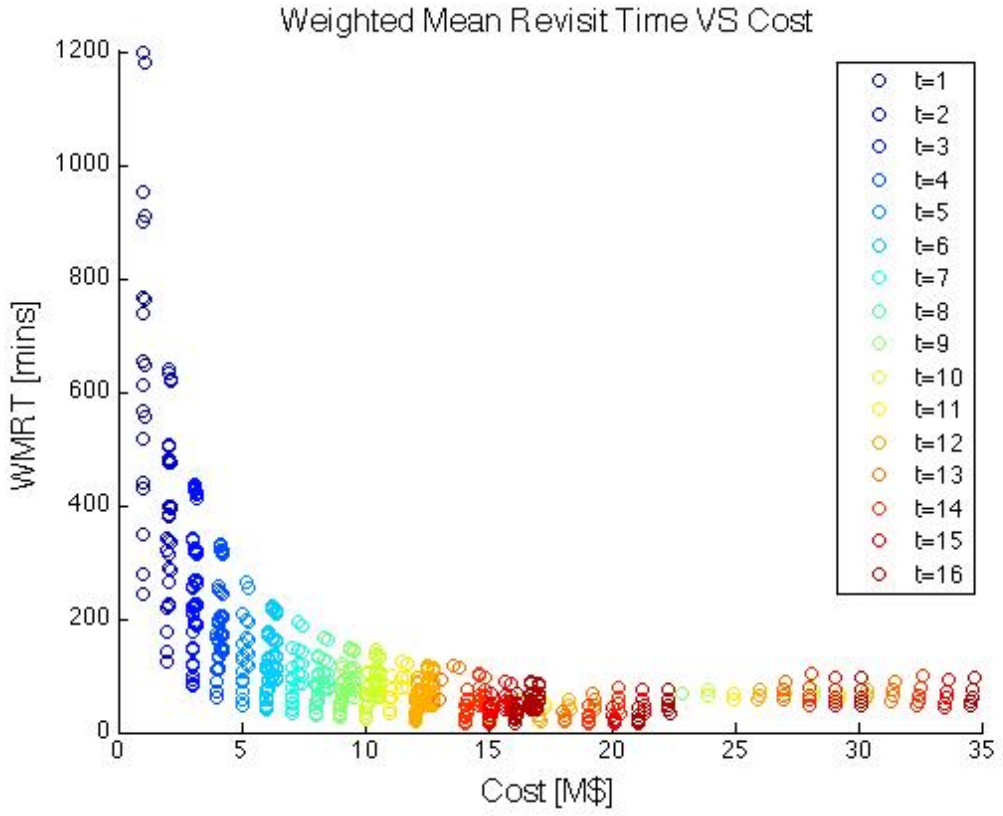

Figure 3.6: Latitude weighted mean revisit time vs cost for all constellations

longest gaps) are much shorter in architectures with 3 planes. This happens for 2 reasons:

- The revisit times CDFs in constellations with just one plane show many short accesses (hence the low low percentiles or even low median if there are many satellites and thus many short gaps) but also very long gaps (hence high high percentiles). However, distributing the satellites in several planes will lead to make the short gaps a bit longer (higher low percentiles) but, at the same time, making the long gaps significantly shorter (lower high percentiles).
- The variability in total number of gaps in different scenarios can affect significantly all the revisit time statistics in the CDF.

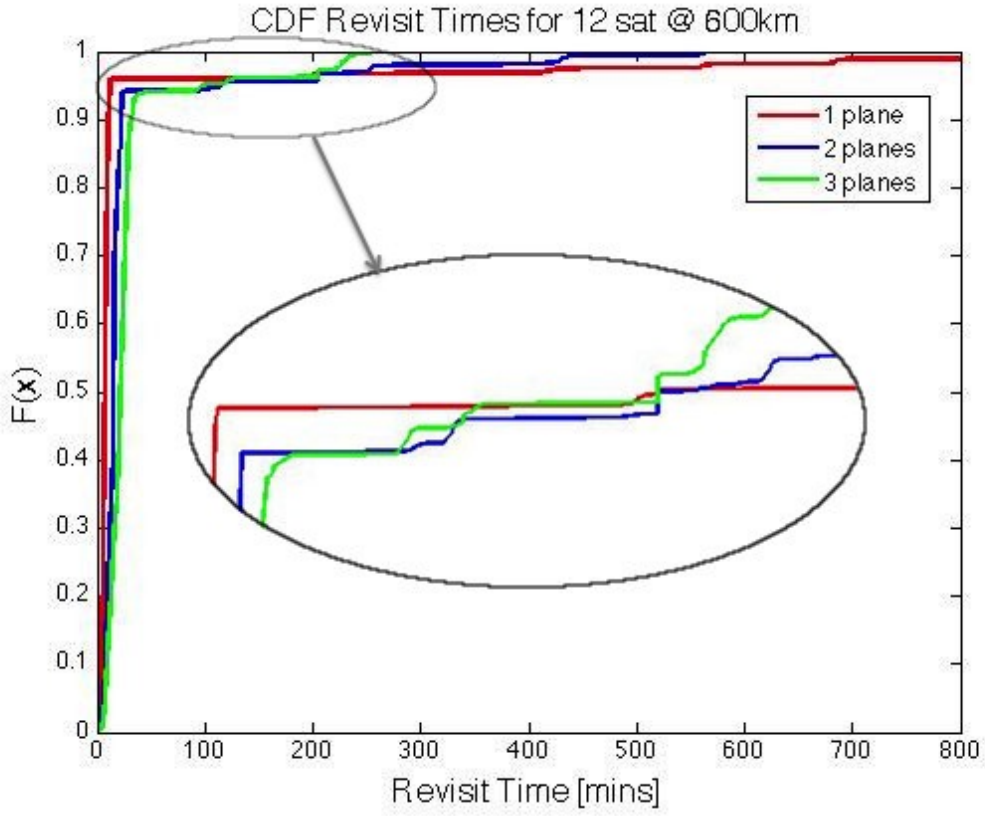

Figure 3.7: Comparison of the CDFs of 3 walker constellations of 12 satellites at 600km altitude and 30 degrees inclination for p = 1, 2 and 3

Moreover, two very sensitive metrics to the selected number of planes are mean response time and the continuous high revisit coverage (CHRC). As it was mentioned in section 2, the former is by definition the average time from when we receive a random request to observe a point until we can actually observe it, and the latter is the percentage of time where the grid point is either in an access or in a gap shorter than a certain threshold, set in our case to 2 hours. In figures 3.9 and 3.10 we can see that distributing the satellites in more than one plane, the time that the constellation will take to access a point after a random request will be shorter than if the satellites were put in a single plane. Likewise, in architectures with just one plane, there is a larger fraction of gaps longer than 2 hours compared to the scenarios where the satellites are distributed in 2 or 3 planes.

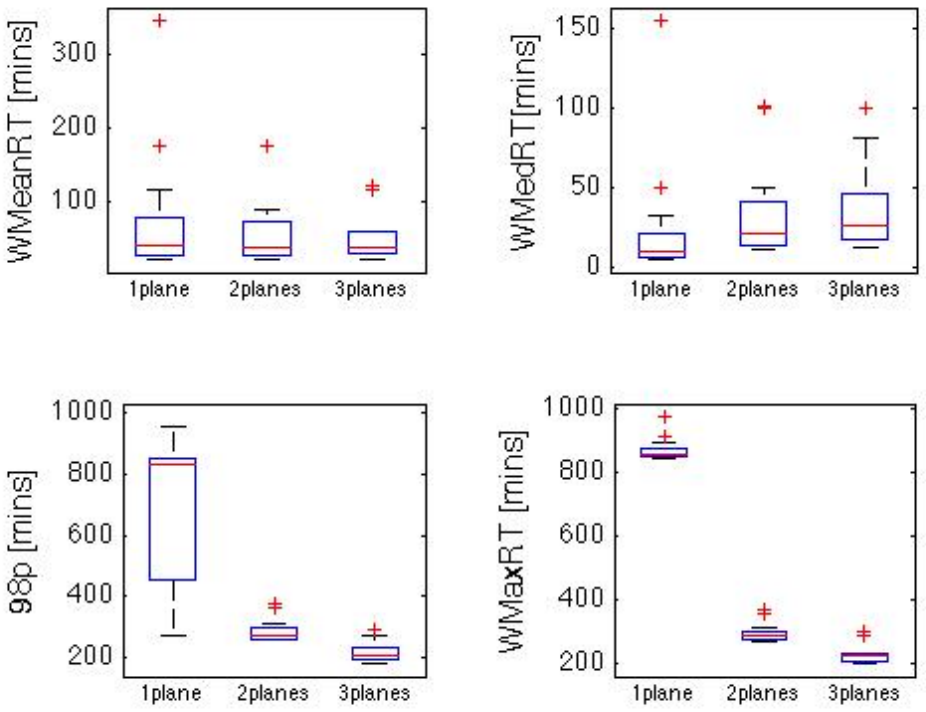

Figure 3.8: Comparison of the latitude-weighted mean, median, 98th percentile and maximum revisit time for different number of planes including all constellations with 30 inclination and 600km altitude

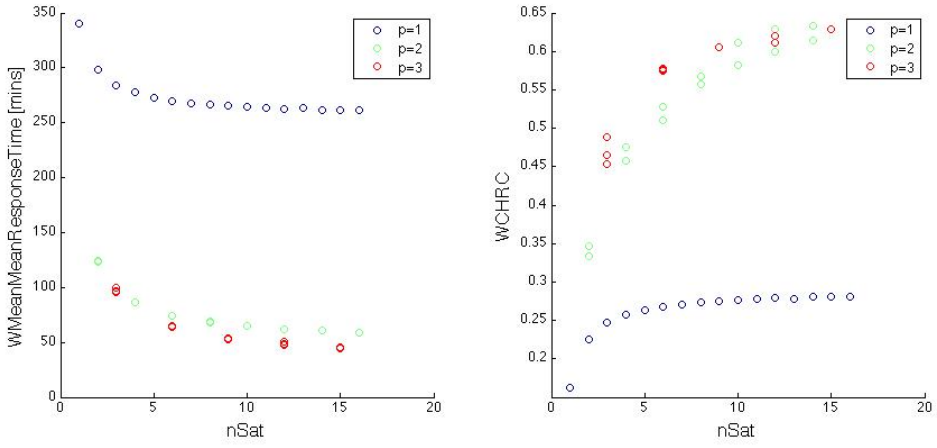

Figure 3.9: Latitude weighted mean response time and Latitude-weighted CHRC_120mins vs nsat for all constellations with 30° inclination and 600km altitude

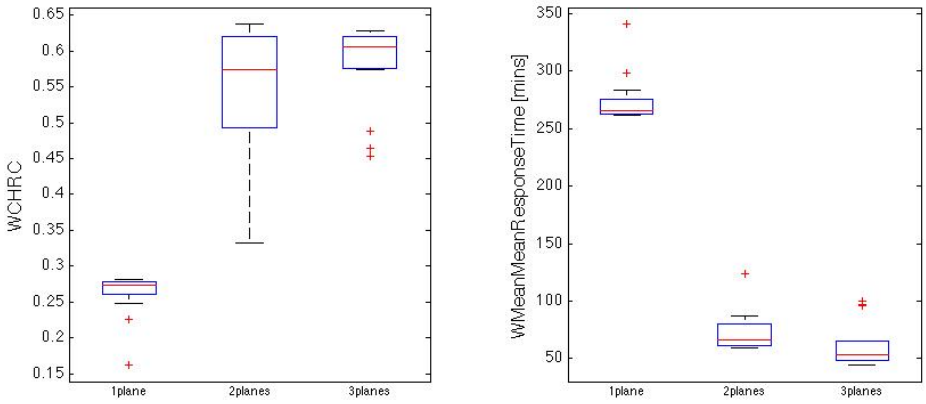

Figure 3.10: Comparison of the latitude-weighted CHRC_120mins and mean response time for different number of planes including all constellations with 30 inclination and 600km altitude

As mentioned in the introductory section 1, since the only requirement set by the TROPICS mission in terms of launch vehicle is to use at most 3 launches (i.e., 3 planes), the increase of cost reflected in our cost model due to adding planes to our constellation loses its relevance. For that reason, and only for the TROPICS mission, the trade-off between the number of planes and cost was ultimately not taken into account. Therefore, distributing the constellation satellites in more than one plane will be preferred to shorten the long gaps and get more desirable revisit times CDFs, as well as mean response time and CHRC values. Furthermore, as it will be detailed later in the section, distributing the satellites in 3 planes provides better coverage performance robustness to LV failures than placing the satellites in just two planes. As shown in figure 3.11, the second mission coverage requirement of having a mean revisit time (unweighted) of 60 minutes or less in the tropics regions is well accomplished by the suggested TROPICS baseline constellation, consisting of 12 satellites distributed in either 2 or 3 different planes equally spaced in RAAN at 600 km and 30 degrees inclination. However, the mean response time metric is significantly better in the

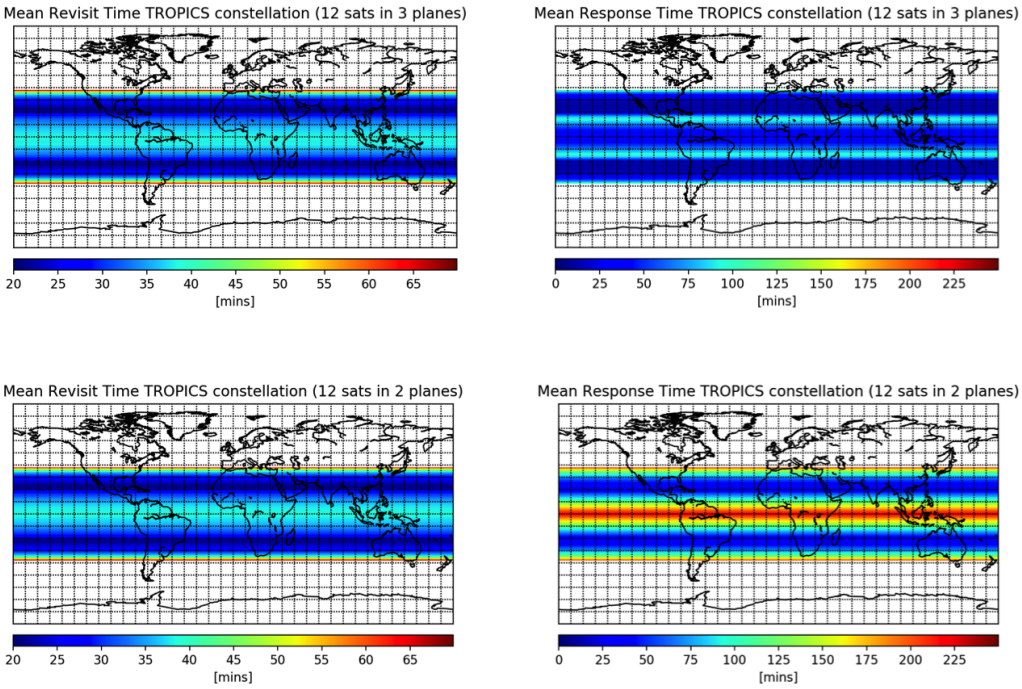

Figure 3.11: Mean revisit time and mean response time heat maps of the baseline constellation of 12 satellites distributed in 3 planes or 2 planes at 600km altitude and 30 degrees inclination

3-plane constellation.

3.3 Robustness characterization

As mentioned previously throughout this thesis, we also wanted to assess the effect/sensitivity of hypothetical operational failures in coverage performance. In particular, we wanted to see how figures of merit such as mean, median and high percentiles of revisit times as well as mean response time change due to satellite losses in the constellation. The degradation of these coverage performance metrics due to successive satellite losses is illustrated in figure 3.12, start-

ing from the baseline architecture with a total number of 12 satellites distributed in 2 or 3 planes. Similarly, figures 3.13 and 3.14 capture the effect of launch vehicle failure on coverage performance for both baseline– i.e. 12 satellites– and threshold– i.e. 6 satellites– architectures. Starting from two constellations of 12 satellites, distributed in 2 and 3 planes equally spaced in RAAN respectively, the degradation of the different coverage metrics is observable with successive satellite losses in the different planes. Note that the planes are indistinguishable from one another since they have identical altitude and inclination values and they are evenly distributed in RAAN. We can notice a significant jump in performance for the transition from a 2-3-3 to a 2-2-3 configuration in the 90th percentile of revisit times. The degradation becomes noteworthy for small constellations with only 5 or 6 satellites where any satellite loss implies a significant decay of coverage performance, especially for the higher percentiles of the gap statistics. Moreover, even though mean revisit times of less than 60 minutes can be accomplished by the threshold configuration with only 6 satellites (seen both in figures 3.4 and 3.12), we can conclude that the 6 satellite configuration is not resilient to even a single satellite loss, since the weighted mean revisit time would go from 59.06 mins to 70.89 mins for the 2-2-2 configuration and from 58.55 mins to 70.4 mins for the 3-3 configuration. However, using the baseline configuration with 12 satellites we could potentially lose up to 6 satellites and still meet the requirement of having a weighted mean revisit time of less than 1 hour. On the other hand, a launch vehicle failure equals to losing an entire orbital plane. Therefore, metrics that are sensitive to the number of planes, such as mean response time and higher percentiles are again the ones mainly affected, as seen in figures 3.13 and 3.14. We can also conclude that the baseline configuration distributed in 3 planes (4-4-4), which has a value of mean revisit

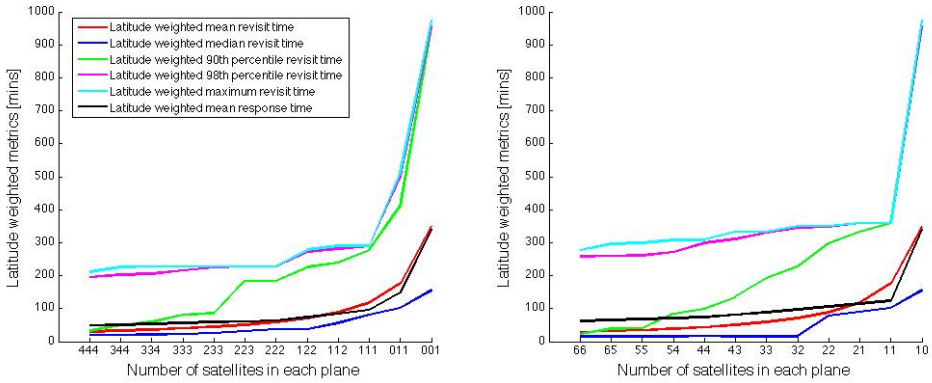

Figure 3.12: Degradation of the latitude weighted metrics due to satellite losses for constellations of 12 satellites distributed in 3 and 2 planes respectively and equally spaced in RAAN at 30 inclination and 600km altitude

time of 29.66 minutes, is resilient to a launch failure and two additional satellite losses, since the 4-4-0 and 3-3-0 configurations have weighted mean revisit time values of 44.37 min and 58.55 min, respectively. Similarly, it is shown that the baseline configuration distributed in 2 planes (6-6), which has a value of mean revisit time of 28.91 minutes, is resilient to a launch vehicle failure since the weighted mean revisit time for the 6-0 configuration is 58.74 min, but the higher percentiles of the gap statistics together with the metrics of mean response time and CHRC would significantly worsen with the resulting 1-plane constellation. Also, the 6-0 configuration does not allow any additional satellite loss to meet the TROPICS mission requirement. Finally, as mentioned previously, threshold configurations (2-2-2 and 3-3) are not resilient to a single satellite loss and, therefore, neither they are to a launch failure, which would imply more than 1 satellite loss.

So far, the satellites and launch vehicle failures have not been modeled using a Bernoulli process as detailed in 2.3. In figures 3.12, 3.13 and 3.14, each point corresponds to just one of the several different possible configurations. For in-

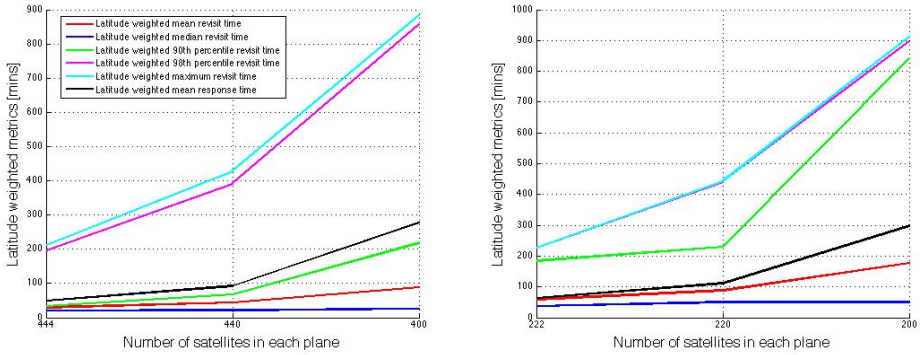

Figure 3.13: Degradation of the latitude weighted metrics due to launch vehicle failure for the baseline and threshold architectures with the satellites distributed in 3 planes equally spaced in RAAN at 30 inclination and 600km altitude

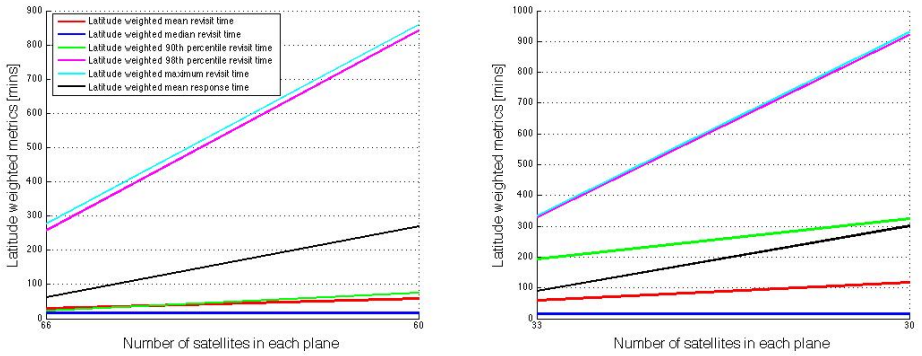

Figure 3.14: Degradation of the latitude weighted metrics due to launch vehicle failure for the baseline and threshold architectures with the satellites distributed in 2 planes equally spaced in RAAN at 30 inclination and 600km altitude

stance, the 3-4-4 constellation can have 4×3 different configurations depending on which of the 12 satellites fails. Even so, each of these points was found to be representative of all the other different possible configurations.

Nevertheless, to account for all the $2^{n_{sat}+n_{planes}}$ different possibilities, the Bernoulli approach was adopted to plot a comparison of the PDFs and CDFs of the weighted mean revisit time metric for the baseline and threshold TROPICS constellations. Doing so, satellite and launch vehicle failures were modeled as a finite sequence of independent and identically distributed binary random

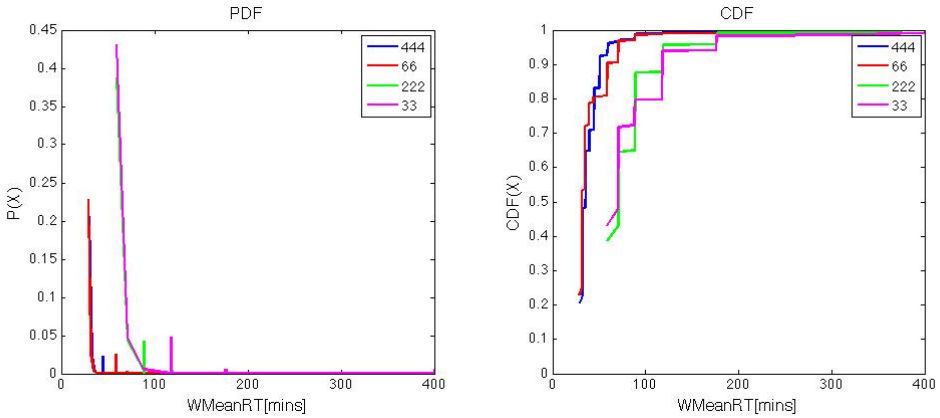

Figure 3.15: Probability Distribution Functions and Cumulative Distribution Functions of weighted mean revisit time for the 4-4-4, 6-6, 2-2-2 and 3-3 constellations at 30 inclination and 600km altitude

variables with a probability of failure of 0.1. The PDFs and CDFs of the 4-4-4, 6-6, 2-2-2, and 3-3 constellations are shown in figure 3.15.

Looking at the CDFs, the robustness of the different constellations can be related to the probabilities of having a weighted mean revisit time of less than 60 minutes, which are 38.74%, 43.05%, 90.56% and 96.27% for the 2-2-2, 3-3, 6-6 and 4-4-4 configurations respectively. Therefore, we can observe the significant increase of coverage performance robustness of the 12-sat baseline architecture with respect to the 6-sat threshold architecture.

3.4 Deployment and lifetime assessment

To complete the TROPICS constellation analysis, we simulate a drag-based deployment strategy to separate satellites in the same orbital plane efficiently. Assuming that all satellites in one plane are deployed in a single launch, it is relevant to assess time required to create the desired Walker constellation geometry, so that all satellites are equally spaced in mean anomaly.

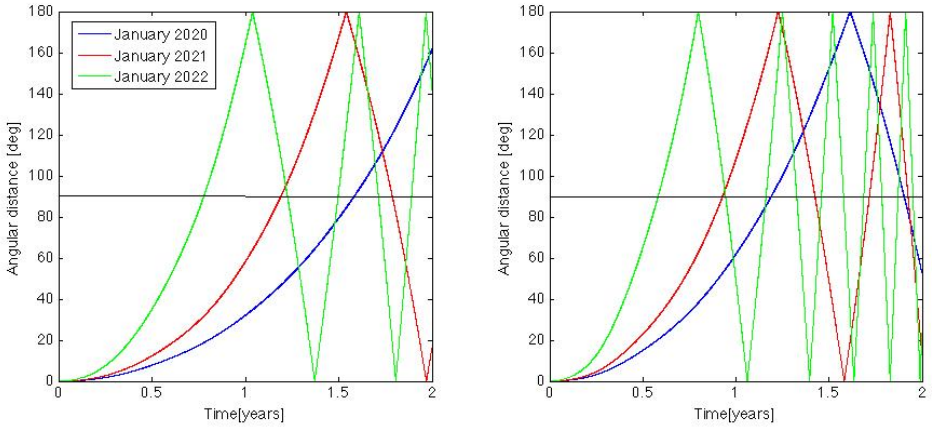

Figure 3.16: Angular separation over time between high drag and low drag satellites at 30° inclination and 600km altitude for the low risk strategy (left) and the high risk strategy (right)

In the deployment strategy considered, every TROPICS CubeSat has 3 different drag states depending on the orientation configuration of the solar arrays shown in table 3.1:

Low Drag	High Drag	Nominal Drag
150 cm^2	1324 cm^2	750 cm^2

Table 3.1: Drag states of the CubeSats

Having two satellites in the same orbital plane and starting off in the same exact position, our deployment strategy consists of setting one satellite to the low drag state and the other one to the high drag state during the eclipse part of the orbit. Both satellites are set to the nominal drag state during the sunlight part of the orbit for power generating purposes. Due to the difference in drag areas, the satellites will slowly drift apart from each other.

However, this deployment strategy involves satellite drag state changes at every eclipse/sunlight event, which entails its correspondent changes in solar panel arrangement. The need for continuous maneuvering of the solar panels

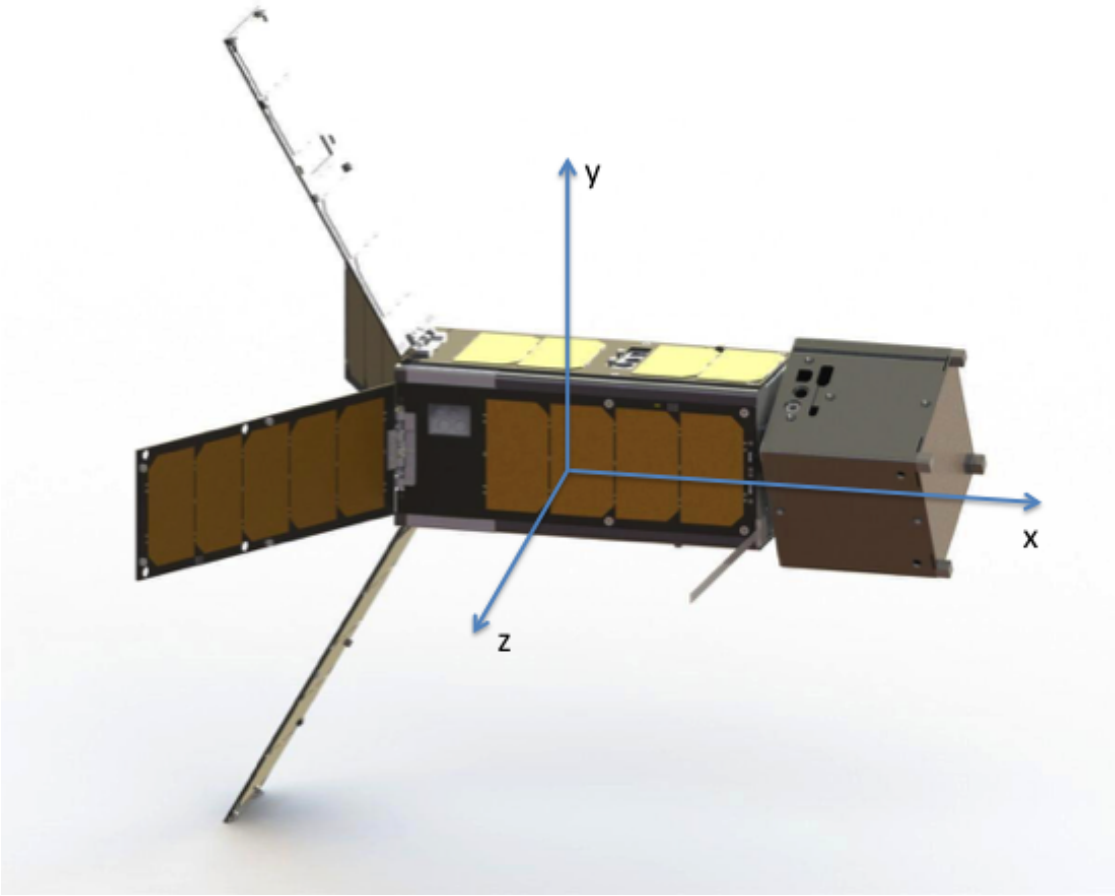

Figure 3.17: Illustration of the MicroMAS-2 satellite deployed to its nominal configuration

was perceived as operationally risky and, therefore, this first strategy has been compared to another one involving less risk. In the second scenario considered, the two satellites are propagated in their minimum (700 cm^2, along the x axis in figure 3.17) and maximum (819 cm^2, along the y or z axis in figure 3.17) drag area once the solar panels are deployed to their nominal configuration (without changes at every eclipse event).

Both simulations were ran for 3 different hypothetical launch dates: January 2020, 2021 and 2022. Figure 3.16 shows that the results change significantly between these three scenarios. This is because, as shown in solar data prediction

400km	500km	600km	700km	800km
0.42 years	6.59 years	21.15 years	>25 years	>25 years

Table 3.2: Satellite's lifetime for different initial altitudes

tables, solar activity starts increasing notably at the beginning of 2021 until 2023 and, therefore, the density of the atmosphere is affected significantly. In the worst case scenario (January 2020 launch date), at 600km and 30° inclination, the time it would take to separate 2 satellites 90 and 180 degrees in mean anomaly would be approximately 1.2 and 1.6 years respectively for the high risk strategy and 1.6 and 2.1 years for the second low risk strategy. On the other hand, in the best case scenario (January 2022 launch date) the time required to separate 2 satellites 90 and 180 degrees in mean anomaly would be approximately 0.6 and 0.8 years respectively for the high risk strategy and 0.8 and 1 years for the second low risk strategy. Again, a trade between risk and deployment performance is observed between the two different strategies considered. In all cases, however, the time to deployment is on the order of months and thus a significant portion of the spacecraft's lifetime.

Finally, we seek to assess if the lifetime of the TROPICS constellation or satellite's de-orbiting time exceeds the NASA's 25 years de-orbiting recommendation[19]. As mentioned in Section 2.4, since this metric depends mostly on the initial altitude of the constellation, satellite lifetimes have been computed for different altitudes and considering a nominal state drag configuration. The results are presented in table 3.2:

These results suggest again that an altitude around 600km is the most suitable one for the TROPICS mission. Constellations with altitudes of 700km or 800km would need to incorporate de-orbiting strategies to fulfill NASA's 25

year lifetime recommendation, as propulsion was deemed not a feasible option for the mission. On the other hand, choosing constellations of 400km or 500km would significantly reduce mission's lifetime due to increase in drag, which implies a faster satellite decay.

CHAPTER 4
CONCLUSION

This work described the process followed to define the constellation and orbit design for the NASA TROPICS mission. In doing so, the different figures of merit used to assess constellation coverage were discussed, and a new metric - continuous high rate revisit coverage - was introduced. Trade-offs between these metrics were discussed. A proxy metric for cost was also introduced that is based on energy considerations and thus independent of the pricing strategy of launch service provider.

For the TROPICS mission, we concluded that 30 degrees inclination architectures provided better coverage metrics for the purpose of monitoring tropical storms. An altitude of 600km was chosen as a compromise between constellation deployment cost, coverage performance, spatial resolution, and lifetime. The number of satellites in the constellation was selected to meet certain mean and median revisit time requirements. We also observed that larger number of planes implies shorter long coverage gaps, getting better higher percentiles statistics of mean revisit times, as well as mean response time and CHRC values.

Another finding for the TROPICS mission is that architectures with several satellites (e.g., 4 per plane) are robust in coverage performance in the sense that degraded constellations in which one or more spacecraft fail are still capable of meeting TROPIC's baseline mission requirements. We also noted that the higher percentiles of revisit times are the metrics most sensitive to hypothetical operational failures.

This work also evaluated the viability of deploying evenly spaced satellites

in the same plane using two strategies based on drag and without using propulsion that show a trade-off between risk and time required to separate satellites in the required geometry.

Finally, the lifetime and orbital decay of satellites was assessed for different altitudes to account for mission life and NASA's 25 year de-orbiting recommendation fulfillment.

While the process laid out in this thesis was adequate for the TROPICS mission, different missions may need to adapt the process to their specific needs, for example by changing the weights in the weighted metrics, using a more specific cost model, or opening the trade space to include non-Walker or hybrid constellations including orbital planes with different altitudes and/or inclinations. However, some of the insights revealed in this work, such as guidelines about how to choose coverage and cost metrics for this process, remain general.

BIBLIOGRAPHY

[1] Ohad Ben-yaacov and Pini Gurfil. Long-Term Cluster Flight of Multiple Satellites Using Differential Drag. 36(6), 2013.

[2] R Bevilacqua and M Romano. Rendezvous Maneuvers of Multiple Spacecraft Using Differential Drag Under J 2 Perturbation. 31(6):1595–1607, 2008.

[3] William J Blackwell, G Allen, C Galbraith, R Leslie, I Osaretin, M Scarito, Mike Shields, E Thompson, D Toher, D Townzen, A Vogel, R Wezalis, Kerri Cahoy, David W Miller, Anne Marinan, Ryan Kingsbury, Evan Wise, Sung Wook Paek, Eric Peters, Meghan Prinkey, Pratik Davé, and Brian Coffee. SSC13-XI-1 MicroMAS : A First Step Towards a Nanosatellite Constellation for Global Storm Observation.

[4] S Bruinsma, G Thuillier, and F Barlier. The DTM-2000 empirical thermosphere model with new data assimilation and constraints at lower boundary : accuracy and properties. 65:1053–1070, 2003.

[5] I-Shih Chang et al. Space launch vehicle reliability. *Crosslink*, 2(1):22–32, 2001.

[6] By Nicholas Crisp, Katharine Smith, and Peter Hollingswort. Small Satellite Launch to LEO : a Review of Current and Future Launch Systems. pages 1–9.

[7] N H Crisp, K Smith, and P Hollingsworth. Acta Astronautica Launch and deployment of distributed small satellite systems $. *Acta Astronautica*, 114:65–78, 2015.

[8] Dominic Depasquale, A C Charania, Spaceworks Commercial, Hideki Kanayama, Seiji Matsuda, Force Application, Launch From, Continental United, Low Earth Orbit, Orbiting Picosatellite, Automated Launcher, Operationally Responsive Space, Polar Satellite, Launch Vehicle, Responsive Access, Small Cargo, Affordable Launch, Spaceworks Engineering, Spaceworks Commercial, Spaceworks Commercial, and Aerospace Policy. Analysis of the Earth-to-Orbit Launch Market for Nano and Microsatellites. (September):1–8, 2010.

[9] Gregory F Dubos and Joseph H Saleh. Comparative cost and utility analysis of monolith and fractionated spacecraft using failure and replacement markov models. *Acta Astronautica*, 68(1-2):172–184, 2011.

[10] T Ely, Rodney Anderson, Y Bar-Sever, David Bell, Joseph Guinn, Moriba Jah, Pieter Kallemeyn, Erik Levene, Larry Romans, and S Wu. Mars network constellation design drivers and strategies. 1999.

[11] Jacob Everist, T Mundhenk, Christopher Landauer, and Kirstie Bellman. Visual surveillance coverage: strategies and metrics. 10 2005.

[12] Matthew Ferringer, Ronald Clifton, and Timothy Thompson. Constellation design with parallel multi-objective evolutionary computation. In *AIAA/AAS Astrodynamics Specialist Conference and Exhibit*, page 6015, 2006.

[13] Matthew Ferringer, Marc DiPrinzio, Timothy Thompson, Kyle Hanifen, and Patrick Reed. A framework for the discovery of passive-control, minimum energy satellite constellations. In *AIAA/AAS Astrodynamics Specialist Conference*, page 4158, 2014.

[14] Matthew P Ferringer, Ronald S Clifton, and Timothy G Thompson. Efficient and accurate evolutionary multi-objective optimization paradigms for satellite constellation design. *Journal of Spacecraft and Rockets*, 44(3):682–691, 2007.

[15] Matthew P Ferringer and David B Spencer. Satellite Constellation Design Tradeoffs Using Multiple-Objective Evolutionary Computation. 43(6), 2006.

[16] Tiffany Finley, Debi Rose, Kyle Nave, William Wells, Jillian Redfern, Randy Rose, and Chris Ruf. Techniques for leo constellation deployment and phasing utilizing differential aerodynamic drag. *Arbor*, 1001:48109–2143, 2013.

[17] Nozomi Hitomi and Daniel Selva. Constellation optimization using an evolutionary algorithm with a variable-length chromosome. In *IEEE Aerosp. Conf.*, 2018.

[18] M Horsley, S Nikolaev, and A Pertica. Small Satellite Rendezvous Using Differential Lift and Drag. 36(2), 2013.

[19] Scott M Hull. End of mission considerations. 2013.

[20] Rocket Lab. Rocket lab launch services.

[21] SEAK Lab. Orbit propagation simulator orekit with seaklab specific functionality. https://github.com/seakers/orekit/tree/dev, 2018.

[22] Erick Lansard, Eric Frayssinhes, and Jean-Luc Palmade. Global design of satellite constellations: a multi-criteria performance comparison of classical walker patterns and new design patterns1. *Acta Astronautica*, 42(9):555–564, 1998.

[23] C L Leonard. Orbital Formationkeeping with Differential Drag. 12(1).

[24] William Mason, Victoria Coverstone-Carroll, and John Hartmann. Optimal earth orbiting satellite constellations via a pareto genetic algorithm. In *AIAA/AAS Astrodynamics Specialist Conference and Exhibit*, page 4381, 1998.

[25] Imane Meziane-Tani, G Métris, Guillaume Lion, Anne Deschamps, Fethi Tarik Bendimerad, and Mohamed Bekhti. Optimization of small satellite constellation design for continuous mutual regional coverage with multi-objective genetic algorithm. *International Journal of Computational Intelligence Systems*, 9(4):627–637, 2016.

[26] Sreeja Nag, Steven P Hughes, and Jacqueline Le Moigne. Streamlining the design tradespace for earth imaging constellations. In *AIAA SPACE 2016*, page 5561. 2016.

[27] Jordi Puig-suari, Guy Zohar, and Kyle Leveque. Deployment of CubeSat Constellations Utilizing Current Launch Opportunities. (805):1–7, 2000.

[28] A Rossi, GB Valsecchi, and P Farinella. Risk of collisions for constellation satellites. *Nature*, 399(6738):743–743, 1999.

[29] Prasenjit Sengupta, Srinivas R. Vadali, and Kyle T. Alfriend. Satellite orbit design and maintenance for terrestrial coverage. 47:177–187, 01 2010.

[30] Solar Flux Unit, Satellite Tool Kit, and I Introduction. Differential Drag as a Means of Spacecraft Formation Control. 47(2), 2011.

[31] Surjit Varma and Krishna Dev Kumar. Mutiple Satellite Formation Flying Using Differential Aerodynamic Drag. 49(2):325–337, 2012.

[32] J.R. Wertz, D.F. Everett, and J.J. Puschell. *Space Mission Engineering: The New SMAD*. Space technology library. Microcosm Press, 2011.

[33] William R Whittecar and Matthew P Ferringer. Global coverage constellation design exploration using evolutionary algorithms. In *AIAA/AAS Astrodynamics Specialist Conference*, page 4159, 2014.

[34] Edwin A Williams, William A Crossley, and Thomas J Lang. Average and maximum revisit time trade studies for satellite constellations using a multiobjective genetic algorithm. *The Journal of the astronautical sciences*, 49(3):385–400, 2001.

[35] Juan Zhang, FengYan Deng, XingSuo He, Liang Li, and Liexia Zhang. Designing leo retrograde orbit satellite constellation for regional coverage, 05 2004.